Modeling Grain Size and Strain Rate in Linear Friction Welded Waspaloy

AHMAD CHAMANFAR, MOHAMMAD JAHAZI, JAVAD GHOLIPOUR,
PRITI WANJARA, and STEPHEN YUE

The high-temperature deformation behavior of the Ni-base superalloy, Waspaloy, using uniaxial isothermal compression testing was investigated at temperatures above the γ' solvus, 1333 K, 1373 K, and 1413 K (1060 °C, 1100 °C, and 1140 °C) for constant true strain rates of 0.001, 0.01, 0.1, and 1 s^{-1} and up to a true strain of 0.83. Flow softening and microstructural investigation indicated that dynamic recrystallization took place during deformation. For the investigated conditions, the strain rate sensitivity factor and the activation energy of hot deformation were 0.199 and 462 kJ/mol, respectively. Constitutive equations relating the dynamic recrystallized grain size to the deformation temperature and strain rate were developed and used to predict the grain size and strain rate in linear friction-welded (LFWed) Waspaloy. The predictions were validated against experimental findings and data reported in the literature. It was found that the equations can reliably predict the grain size of LFWed Waspaloy. Furthermore, the estimated strain rate was in agreement with finite element modeling data reported in the literature.

I. INTRODUCTION

WASPALOY is a wrought Ni-base superalloy commonly used as blade and disk material in jet engines and land-based gas turbines due to its high-temperature strength and corrosion resistance.[1] This alloy gains its high-temperature strength during post-forge heat treatment through precipitation of γ', Ni$_3$(Al, Ti), particles with a volume fraction of 30 pct and solvus of 1303 K (1030 °C).[2,3] Also, alloying elements such as Cr, Co, and Mo provide additional strength by solid solution strengthening.[4,5] Titanium-, Mo-, and Cr-based carbides supply further strength through pinning of grain boundaries and thereby decreasing the grain boundary sliding at high temperatures.[5] Chromium and Al in Waspaloy form the protective Cr$_2$O$_3$ and Al$_2$O$_3$ oxide layers which are critical for the oxidation and corrosion resistance of the alloy.

Linear friction welding (LFW) is a solid-state joining technology which is being considered for joining of blades to disks, since it offers significant advantages over the existing technologies such as mechanical joining or machining of bladed integrated disks (blisks) from solid forged billets.[6] In LFW, the two surfaces to be welded together are brought into contact and subjected to an axial pressure. While one of the parts is stationary, a reciprocating movement is imposed on the second one. The oscillatory movement under axial pressure results in significant temperature increase in the interface and thus material softening. Once enough softening has taken place at the interface, the oscillating part is aligned with the stationary part, and the pressure is maintained or increased to consolidate the two parts together. During the LFW process, the interface material is subjected to high strain rate deformation at high temperatures, and some amount of the plasticized material is expelled to the sides as flash. In some aspects, the LFW process is similar to a high strain rate forging process in which axial shortening generates the flash. Temperature, strain, and strain rate are the three critical factors influencing the microstructure and quality of a linear friction-welded (LFWed) joint. Of particular importance is the significant change in grain size in the weld area because of the occurrence of dynamic recrystallization (DRX). The prediction and control of the grain size in the weld area are very important factors to attain the required creep, stress rupture, and crack growth resistance.

However, reliable estimation of temperature, strain, and strain rate is one of the major challenges for studying grain size evolution during the LFW process. Indeed, because of high-frequency oscillation, material removal due to wear, and material expulsion as flash,

AHMAD CHAMANFAR, Postdoctoral Fellow, formerly with the Department of Materials Engineering, McGill University, 3610 University Street, Montreal, QC H3A 0C5, Canada and Metallic Products Manufacturing, National Research Council Canada Aerospace, 5145 Decelles Avenue, Montreal, QC H3T 2B2, Canada, is now with the Département de Génie Mécanique, École de Technologie Supérieure, 1100 rue Notre-Dame Ouest, Montreal, QC H3C 1K3, Canada. Contact e-mail: ahmad.chamanfar@mail.mcgill.ca MOHAMMAD JAHAZI, Professor, is with the Département de Génie Mécanique, École de Technologie Supérieure. JAVAD GHOLIPOUR, Research Officer, and PRITI WANJARA, Group Leader, are with the Metallic Products Manufacturing, National Research Council Canada Aerospace. STEPHEN YUE, Professor, is with the Department of Materials Engineering, McGill University.

the interface temperature cannot be measured directly by placing embedded thermocouple probes. Moreover, because of *local* severe plastic deformation at the weld interface, the strain and strain rate experienced by the interface material cannot be determined using strain gauges. Similarly, because of flash development and geometric constraints due to the use of holders for the two welding parts, the strain rate cannot be measured using high-speed cameras since the camera does not have line of sight for the interfacial region. Therefore, various researchers have attempted to calculate or model the strain rate evolution in the LFW process.[7,8] However, no general agreement exists in the reported values, and large discrepancies between the calculated and modeled values have been reported.[7]

A better understanding of grain size evolution during LFW becomes even more important when process simulation of industrial-size components with complex geometries is considered. Such simulations can only be fully exploitable when they are based on reliable constitutive equations describing the evolution of the microstructure, specifically the grain size, during the LFW process. Such equations are often generated based on hot compression testing relating the evolution of the grain size to strain rate and temperature of deformation.

In the published literature, the available data on hot deformation of Waspaloy are limited to number of testing conditions.[9–11] The only equation for grain size evolution in Waspaloy during hot deformation is the one proposed by Shen *et al.*[12] obtained from Gleeble compression testing. At the beginning of the current study, attempt was made to compare the measured grain size of isothermally hot compressed Waspaloy with the calculated one using the equation proposed in Reference 12. The measured grain sizes for different testing conditions were significantly different from the calculated ones. For example, for the isothermal hot compression temperature of 1373 K (1100 °C), strain rate of 1 s^{-1}, and strain of 0.83, the measured grain size was 27.7 μm, whereas a grain size of 16.8 μm was obtained using the proposed equation. The differences are probably due to the different nature of equipment used in that study. In fact, as noted by the authors,[12] Gleeble compression testing is characterized by a significant axial temperature gradient from the end of the sample toward the mid-height, resulting in a sharp gradient in the grain size along the height of the sample. Considering the material removal for metallography preparation, it is difficult to measure the grain size at the same *exact* spot for each test to insure the same evaluation for the grain size determination. It must be also noted that the microstructure of the hot-compressed Waspaloy has been rarely presented in the literature. This may be because of difficulties encountered in revealing the grain boundaries of hot deformed Waspaloy. Lack of such data is an important impediment in the reliable estimation of the grain size and morphology as a function of deformation conditions.

Hence, in the early stages of the current study, a method was developed, which allows for a reliable and repeatable revealing of grain boundaries in hot-deformed Waspaloy. Isothermal compression testing over a wide range of temperatures and strain rates was carried out to study the microstructural development in Waspaloy and determine the constitutive equations for grain size evolution. Specifically, since the weld area is exposed to supersolvus temperatures, greater than 1303 K (1030 °C) during LFW,[2] the focus was on hot compression in this temperature range. The developed constitutive equations were then used to predict the grain size in LFWed Waspaloy. For grain size predictions, the interface temperature was estimated using a one-dimensional transient-heat-conduction analysis. The strain rate in LFW was estimated using a new approach which was based on the development of the constitutive equations for grain size evolution during hot deformation and grain size measurements under various LFW conditions. Finally, since γ' is the main phase for grain size control during thermomechanical processing of Waspaloy, the evolution of this phase during the current experimental work was also investigated.

II. EXPERIMENTAL MATERIAL AND PROCEDURES

The samples for hot compression experiments and LFW were extracted from an as-received Waspaloy disk. The disk was in solution heat-treated and double-aged condition with a hardness of 420 ± 5 HV. The chemical composition of the disk was determined to be (wt pct): Ni-17.08Cr-12.87Co-1.00Fe-4.12Mo-3.35Ti-1.07Al-0.07B-0.01Zr-0.04C.

For hot compression testing, cylindrical samples with dimensions of 6 mm in diameter and 9 mm in height were prepared by wire electro-discharge machining from the disk. For conducting the uniaxial hot compression tests, a computer-controlled 250 kN servo-hydraulic MTS testing machine equipped with a radiant cylindrical furnace was used. The furnace was capable of keeping the temperature of the sample, tools, and surrounding atmosphere within ±5 K (5 °C). During the tests, the temperature of the radiant furnace, containing the tools and the sample, was raised to 1273 K (1000 °C) at a heating rate of 1.5 K/s (1.5 °C/s) and then to 1373 K (1100 °C) at the rate of 0.5 K/s (0.5 °C/s). After holding for 15 minutes at 1373 K (1100 °C) (solutionizing), the sample was heated or cooled to the deformation temperature at the rate of 0.5 K/s (0.5 °C/s). The sample was held at the deformation temperature for 5 minutes to insure temperature uniformity. Afterward, deformation to a strain of 0.83 was applied at a constant strain rate, and then the sample was water quenched to retain the deformed microstructure. The studied deformation temperatures were supersolvus, *i.e.*, 1333 K, 1373 K, and 1413 K (1060 °C, 1100 °C, and 1140 °C). The applied strain rates were 0.001, 0.01, 0.1, and 1 s^{-1}. Graphite, mica sheet, and boron nitride were used as lubricant layers between the sample and anvils during the hot compression tests. A K-type thermocouple in contact with the sample was employed to control the temperature during the test using a digital controller. To conduct the hot deformation at a constant strain rate, the

crosshead speed was adjusted by means of the displacement of the lower actuator and the control software of the MTS equipment. Furthermore, in the current study, the sample and dies were enclosed in a quartz tube through which a constant flow of argon gas was passed to increase the temperature uniformity of the sample and to minimize oxidation of the sample and tools.

For the LFW experiments, rectangular blocks with dimensions of $13 \times 11 \times 18$ mm^3 (length $\times$ width $\times$ height) were wire electro-discharge machined from the same disk from which the hot compression samples were prepared. LFW was conducted in air at room temperature using an MTS LFW process development system, with the oscillation being applied perpendicular to the cross section defined by the width and height. The main components of the LFW machine are two hydraulic actuators; the lower in-plane actuator that oscillates the bottom joint half in the horizontal direction and the forge actuator that applies a downward pressure on the top stationary part.

In a previous study by the authors of the current study,[13] it was shown that axial shortening, the total amount of reduction in height in the LFW samples at the end of LFW, can be used as a reliable indication of the combined effects of frequency, amplitude, pressure, and welding time. The same approach was used in the current study, and the data reported in Table I show the LFW processing conditions and the corresponding axial shortening values.

For metallographic analysis, the quenched hot compression samples were sectioned parallel to the compression axis at mid-diameter. Linear friction-welded (LFWed) samples were cut along the height $\times$ length plane, at mid-width. For cutting the samples, a precision abrasive alumina oxide cut-off wheel was employed. Automated grinding and polishing procedures were used to prepare the samples for microstructural examination by optical microscopy (OM) and scanning electron microscopy (SEM). For the OM studies on the parent disk material, after ultrasonic cleaning, the polished samples were immersion etched for 5 seconds in a solution composed of 60 mL HCl, 40 mL HNO$_3$, and 40 mL CH$_3$COOH.[14] For the OM studies on the solution heat-treated, hot-compressed, and LFWed samples, the polished surfaces were electroetched in a solution composed of 10 g oxalic acid in 100 mL deionized water[15] with voltages ranging from 5.5 to 6.5 V at a current of 0.1 A for period ranging from 8 to 42 seconds, depending on the processing conditions. SEM studies for γ' particles characterization were carried out using a high-resolution Hitachi S-4700 Field Emission Gun (FEG) SEM operated at an accelerating voltage of 15 kV in secondary electron (SE) mode. The samples for SEM investigations were electroetched at room temperature for 3 seconds in a solution of 0.4 g

CrO$_3$, 42 mL H$_3$PO$_4$, and 2.5 mL H$_2$SO$_4$ with a voltage of 3 V at a current of 0.1 A.[16]

The γ grain size and γ' particle size were measured using the Clemex® image analysis software. The volume fraction of γ' was determined based on ASTM E 562-02 standard.[17] To increase reliability of the data and obtain statistically representative results for the average γ grain size, γ' mean particle size, and percent volume fraction of γ', at least six micrographs were examined. In order to determine the γ grain size, more than 200 grains were sampled from each OM image. For measurements of the primary and secondary γ' sizes, 28 and 101 particles were considered, respectively.

III. RESULTS AND DISCUSSION

A. The Activation Energy for Hot Deformation

The true stress–strain curve calculated from the load–displacement data collected during compression testing and corrected for the effects of friction and adiabatic heating[18] are presented in Figure 1 for the testing temperature of 1333 K (1060 °C) and different strain rates. Based on this figure, after the elastic region, a work hardening region is observed; the plastic flow stress increases with strain up to a peak value. In this region, the dislocation generation rate is higher than the dislocation annihilation rate caused by dynamic recovery (DRV). Since DRV is sluggish in Ni-base superalloys because of their low stacking fault energy, after a critical strain is surpassed, the high density of dislocations encourages the onset of DRX at strains roughly equal to 0.8 of the strain at the peak stress. After the peak stress, flow softening
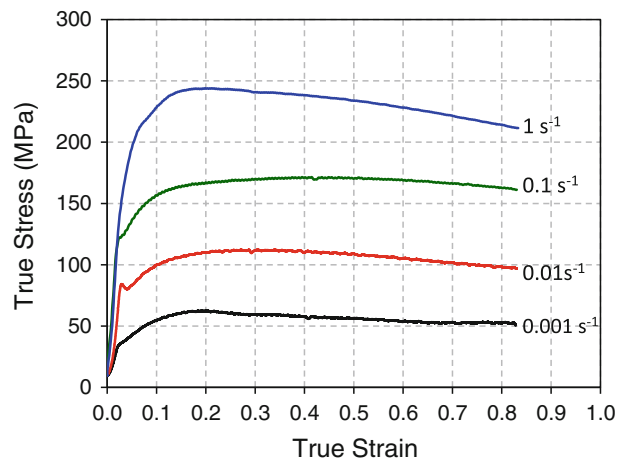

Fig. 1—Variation of flow stress with strain at temperature of 1333 K (1060 °C) and different strain rates. The flow stress was corrected for the friction and adiabatic heating effects.

Table I. LFW Processing Conditions in the Current Study

Sample ID	Oscillation Pressure	Forge Pressure	Axial Shortening (mm)
A	1P	1P	1.2
B	1.3P	4P	4.6

occurs, and the stress decreases continuously with further increase in the strain because of the progress of DRX. For strain rates of 0.001, 0.01, and 0.1 s^{-1}, flow softening proceeded until a near-steady-state stress was achieved at a strain of about 0.83. Steady state indicates the completion of DRX, *i.e.*, the rate of dislocation generation is the same as the DRX rate. In contrast, for strain rate of 1 s^{-1} the above near-steady-state behavior was not observed.

The following constitutive equation is often used for relating the flow stress (σ) to deformation temperature (T) and strain rate ($\dot{\varepsilon}$) in Ni-base superalloys[18,19]:

$$\sigma = A\dot{\varepsilon}^m \exp\left(\frac{mQ}{RT}\right) \quad [1]$$

where A, m, Q, and R are, respectively, the material constant, the strain rate sensitivity, the activation energy for hot deformation, and gas constant. The m and Q parameters can be determined as follows:

$$m = \left.\frac{\partial \ln \sigma}{\partial \ln \dot{\varepsilon}}\right|_T \quad [2]$$

$$Q = \frac{R}{m} \left.\frac{\partial \ln \sigma}{\partial (1/T)}\right|_{\dot{\varepsilon}}. \quad [3]$$

Considering the stress at a strain of 0.83, ln σ *vs* ln $\dot{\varepsilon}$, and ln σ *vs* $1/T$ were plotted in Figure 2 for the different hot compression conditions used in the current study. It can be seen that the flow stress increases with increasing strain rate and decreasing temperature. Furthermore, the slopes of the regressions are independent of temperature and strain rate, respectively. With determination of the slopes of the regressions, the m and Q parameters were calculated to be 0.199 ± 0.008 and 462 ± 95 kJ/mol, respectively, using Eqs. [2] and [3]. The determined value of Q is consistent with the value of 410 kJ/mol reported by McQueen *et al.*[10] for hot deformation of Waspaloy in the temperature range of 1173 K to 1473 K (900 °C to 1200 °C).

B. *Occurrence of DRX During Hot Compression of Waspaloy*

Figure 3 shows the microstructure of the as-received material. The microstructure consisted of fine equiaxed γ grains with an average size of $10 \pm 1~\mu m$, as shown in Figure 3(a). SEM studies, Figure 3(b), reveals the presence of primary and secondary γ' precipitates with average diameters of 250 ± 35 and 43 ± 19 nm, respectively, and a combined total volume fraction of 30 pct. As noted in Figure 3(b), carbides with a size of 35 ± 27 nm and a total volume fraction of 0.5 pct were also identified in the initial microstructure.

Grain size measurements on the samples quenched just before the start of deformation at 1333 K (1060 °C), showed that the grain size of the starting material increased from 10 ± 1 to $211 \pm 10~\mu m$, clearly indicating that grain growth had taken place (Figure 4(a)). The objective of the solution heat treatment was to dissolve the γ' precipitates to obtain a similar microstructure to the
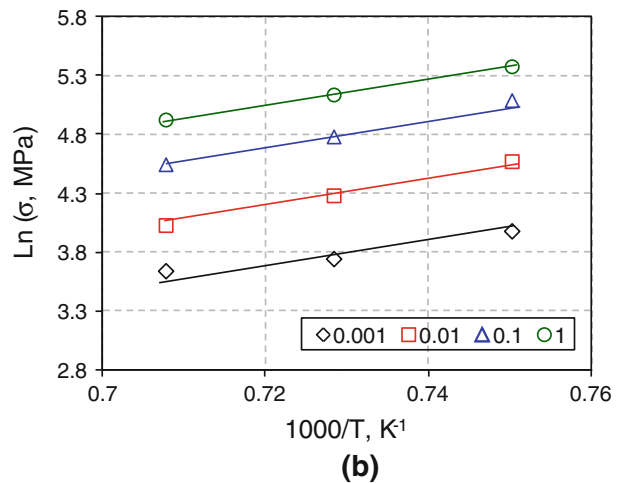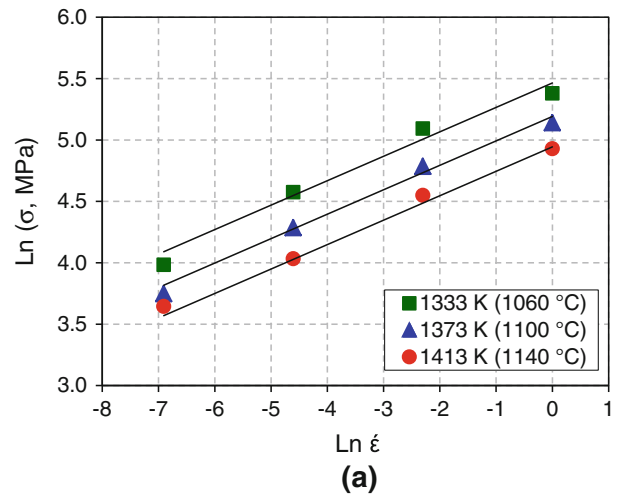

(a)

(b)

Fig. 2—Variation of (*a*) ln σ *vs* ln $\dot{\varepsilon}$ and (*b*) ln σ *vs* $1/T$ during supersolvus deformation of Waspaloy.

one observed in the LFWed joints, in which almost complete γ' dissolution occurred in the weld area.[2] Solution heat treatment of the samples extracted from the disk (*i.e.*, 15 minutes at 1373 K (1100 °C) plus cooling to the deformation temperature of 1333 K (1060 °C) and holding at this temperature for 5 minutes) revealed that γ' particles had dissolved completely, and only the MC type carbides with irregular morphology remained, Figure 4(b). Therefore, at deformation temperatures greater than the γ' solvus, *i.e.*, above 1303 K (1030 °C), the dislocation density, solutes, and MC type carbides are the factors contributing to the flow stress of the alloy. It is worth noting that the observed grain growth in the solution heat-treated sample may be related to the absence of γ' particles dissolved as a result of the solution heat treatment.

The microstructure of the sample subjected to 0.83 strain at a deformation temperature of 1333 K (1060 °C) and a strain rate of 1 s^{-1} is shown in Figures 5(a) and (b), as an example. The microstructure was not fully dynamically recrystallized, consistent with the flow curve. However, significant grain refinement, compared with the microstructure before starting the deformation (Figure 4(a)), occurred because of DRX; the grain size

was reduced from 211 ± 10 to 27 ± 1 μm. With increasing deformation temperature to 1413 K (1140 °C), the microstructure was almost fully recrystallized (Figures 5(c) and (d)), though the grains were coarser (44.1 ± 0.4 μm) compared with that at 1333 K (1060 °C).

C. Variation of Grain Size with Zener–Hollomon Parameter

The variation of the dynamic recrystallized (DRXed) grain size with the process parameters can be correlated using the Zener–Hollomon parameter (Z), expressed as[20]

$$Z = \dot{\varepsilon} \exp\left(\frac{Q}{RT}\right). \qquad [4]$$

The activation energy obtained in the current investigation, 462 kJ/mol, was used to calculate the Z parameter for different hot compression conditions. The Z parameter was used to relate the grain size to the hot compression temperature and strain rate at a strain of 0.83, as shown in Figure 6. Two distinct regimes were identified; low and high strain rate regimes. In the low strain rate regime, the evolution of the grain size with Z for strain rates equal to and less than 0.1 s^{-1} is presented, while in high strain rate regime that for strain rate of 1 s^{-1} is displayed. Exceptionally, for strain rate of 0.1 s^{-1} and deformation temperature of 1413 K (1140 °C), the relationship of ln d vs ln Z followed that of the high strain rate regime.

The dependency of the grain size on the strain rate can be related to the deformation mechanisms. At strain rates ≤0.01 s^{-1}, the deformation is uniform, and the deformed microstructure exhibits a typical DRXed microstructure (Figure 7). In other words, for a low strain rate regime, DRX is the main deformation mechanism and initiates preferentially at the prior grain boundaries. In contrast, based on TEM observations with increasing strain rate to 1 s^{-1}, deformation becomes localized and mechanical twins form adjacent to the grain boundaries.[21] The twin boundaries are composed of piled-up dislocations, and DRX initiates near them as well as at the prior grain boundaries. Thus,
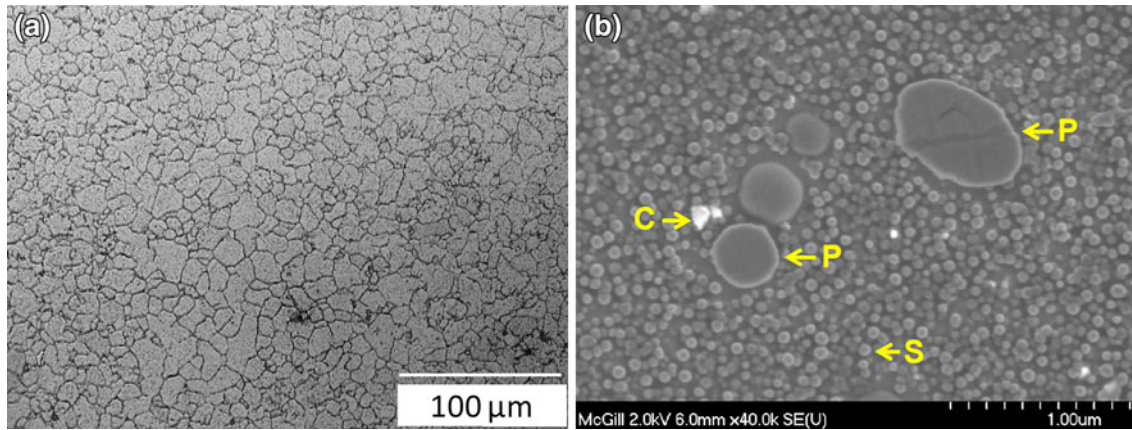

Fig. 3—Initial microstructure of the compression samples extracted from the disk; (a) optical microscopy image, (b) SEM micrograph presenting the primary γ', secondary γ', and carbides (marked by P, S, and C, respectively).
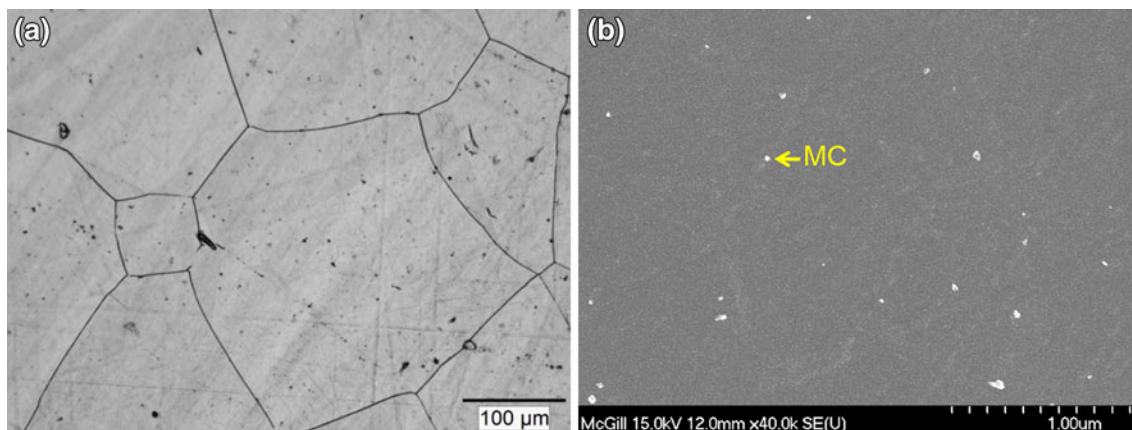

Fig. 4—Microstructure of the compression sample quenched just before starting deformation at 1333 K (1060 °C): (a) optical micrograph, (b) SEM image: white remaining precipitates are MC type carbides.
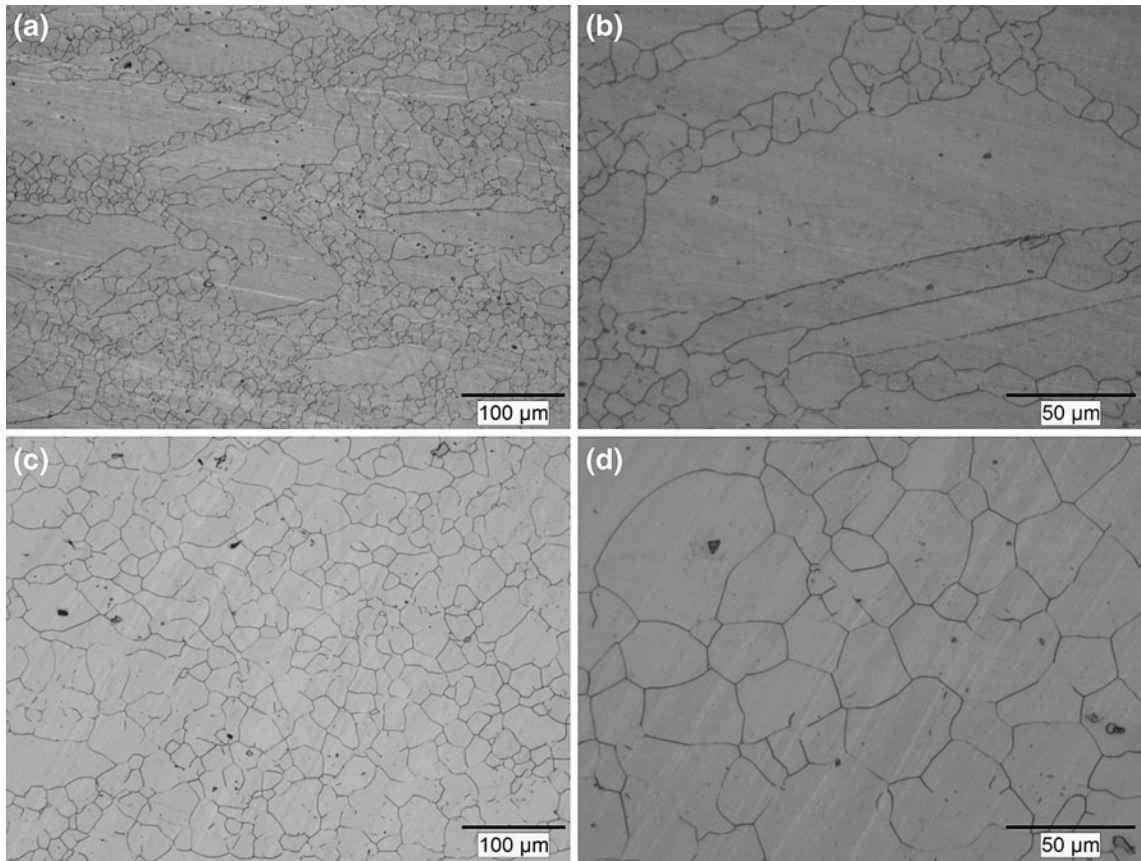
Fig. 5—Microstructure of the compression sample deformed to a true strain of 0.83 with a strain rate of 1 s^{-1} at a deformation temperature of (*a*) and (*b*) 1333 K (1060 °C), and (*c*) and (*d*) 1413 K (1140 °C).
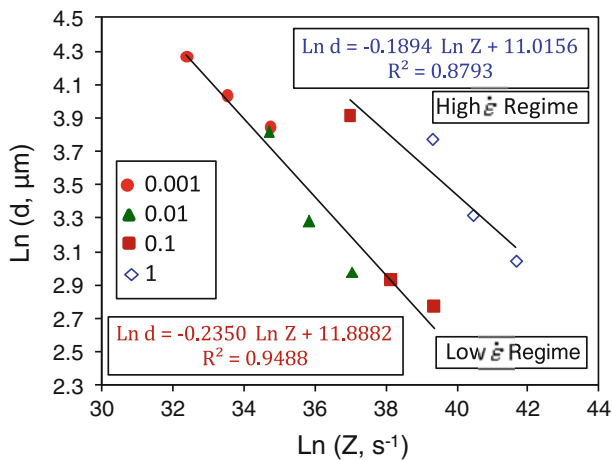

Fig. 6—Variation of the grain size with the Zener–Hollomon parameter in Waspaloy.

Fig. 7—Microstructure of the sample deformed at 1373 K (1100 °C) to a strain of 0.83 at a strain rate of 0.01 s^{-1}.

for the high strain rate regime, mechanical twins in addition to dislocation slip are probably the dominant deformation mechanisms.[21] For strain rate of 0.1 s^{-1} and deformation temperature of 1413 K (1140 °C), the deformation mechanisms are probably the same as those for the high strain rate regime. However, this issue is currently under investigation.
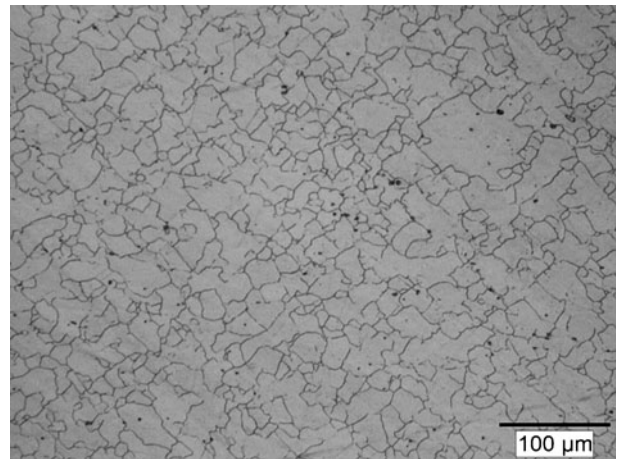
The results of Figure 6 indicate that, the grain size decreases continuously with increasing Z parameter, and their relationships for low and high strain rate regimes can be, respectively, formulated as

$$\ln d = -0.2350 \ln Z + 11.8882 \qquad [5a]$$

$$\ln d = -0.1894 \ln Z + 11.0156. \qquad [5b]$$

D. Prediction of Grain Size and Strain Rate in LFWed Waspaloy

In order to predict the grain size of the weld interface, the temperature at the interface and the corresponding strain rate should be known. Owing to severe plastic deformation at the weld interface, the interface temperature cannot be directly measured by placing thermocouples. The authors of the current study demonstrated in a previous study[2] that a reliable estimation of the temperature at the interface can be made using a one-dimensional transient-heat-conduction analysis.

Evaluation of the strain rate during LFW is another technical and scientific challenge. Vairis and Frost[8] proposed the following equation for strain rate in the weld area in LFW:

$$\dot{\varepsilon} = \frac{af}{L} \qquad [6]$$

in which a, f, and L are, respectively, the amplitude, the frequency of oscillation, and the length of the LFW sample. Also, Turner et al.[7] estimated the strain rates for different amplitudes of oscillations using finite element modeling (FEM). The large difference between the calculated strain rate (1 s^{-1}) using Eq. [6] and FEM-based estimation (1000 to 1500 s^{-1}) for LFW of Ti-6Al-4V[7] is indicative of the uncertainty in the actual value of the strain rate during LFW. In the current investigation, the measurement of the grain size and the development of the constitutive equations are used as a new approach for estimating the strain rate during the LFW process.

The microstructures of the weld interface in weldments A and B are shown in Figure 8, with an average grain size of 13.1 ± 0.3 and 4.0 ± 0.1 μm, respectively. The predicted results for the grain size at the weld interfaces of weldments A and B are compared with the experimental measurements in Table II. In the calculation, the temperature was estimated using a one-dimensional transient-heat-conduction analysis described in Reference 2, and the strain rate was estimated from Eq. [6] as well as from the model described in Reference 7. Using the constitutive equation for the high strain rate regime, Eq. [5b], and strain rate from the model described in Reference 7, a very good agreement (2.9 pct difference) was obtained between the predicted (13.4 μm) and the measured (13.1 μm) grain sizes for weldment A as shown in Table II. This can be explained with a more in-depth analysis of the LFW process:

a) As shown in Figure 9(a), for weldment A, almost the entire deformation occurs in the oscillation phase. Interestingly, Turner et al.[7] prediction for strain rate is for the oscillation phase of the LFW process. Similarly, the transient-heat-conduction analysis estimates the temperature for the end of
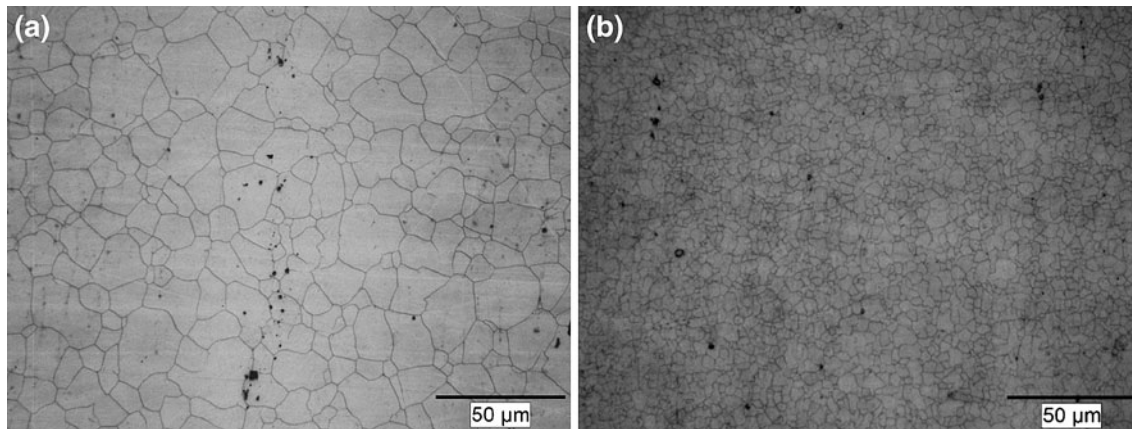

Fig. 8—Microstructure of the weld interface in LFWed (a) sample A and (b) sample B, with an average grain size of 13.1 ± 0.3 and 4.0 ± 0.1 μm, respectively.

Table II. Comparison of Grain Size Predictions with Measurements at the Weld Interface of Weldments A and B

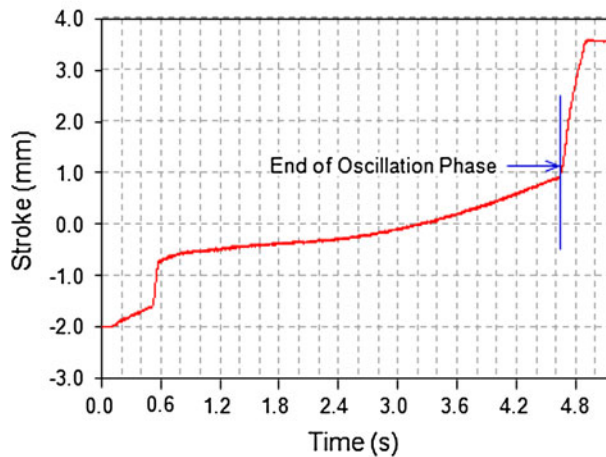| Sample ID	Interface Temperature [K (°C)]*	Strain Rate (s^{-1})	Modeled Grain Size, Eq. [5a] (μm)	Modeled Grain Size, Eq. [5b] (μm)	Measured Grain Size (μm)
A	1491 (1218)	18.5**	11.7	30.2	13.1
A	1491 (1218)	1325†	4.3	13.4	13.1
B	1577 (1304)	15.4**	19.5	46.0	4.0
B	1577 (1304)	825†	7.7	21.6	4.0

*Estimated from one-dimensional transient-heat-conduction analysis.
**Vairis and Frost equation.
†Turner's modeling.
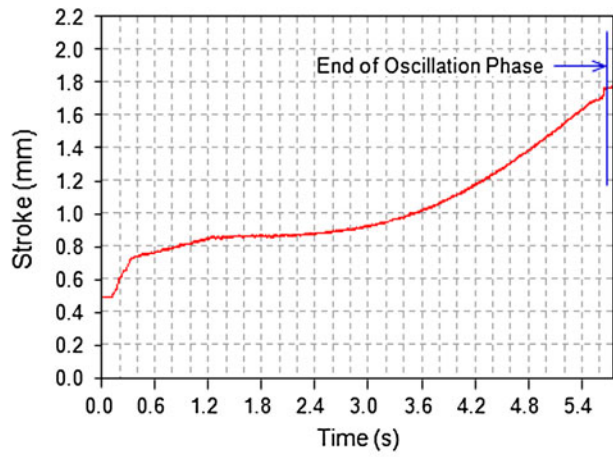
Fig. 9—Variation of stroke with time during LFW of weldments (*a*) A and (*b*) B.

Fig. 10—Variation of the cooling rate as a function of distance from the weld interface in weldment A.

the oscillation phase. Thus, the thermomechanical conditions (temperature and strain rate) of the interface material were estimated reliably, and consequently the grain size was predicted consistently. In other words, reliable inputs were given into the constitutive equation, and a reliable output was obtained.

b) Figure 10 shows the cooling rate *vs* location from the weld interface during LFW of weldment A determined by placing thermocouple probes at different locations from the weld interface. By extrapolating the data of Figure 10, the cooling rate at the weld interface can be estimated to be about 82 K/s (82 °C/s). Thus, after completion of the oscillation phase, the temperature of the interface drops rapidly (within about 9 seconds) from 1491 K (1218 °C), Table II, to 773 K (500 °C). According to the Hu *et al.* study,[22] this time period is too short for significant changes in the grain size to take place as a result of occurrence of meta-dynamic recrystallization (MDRX), static recrystallization (SRX), and grain growth. As part of the experimental process, upon the completion of the hot compression test, the sample was quenched in a
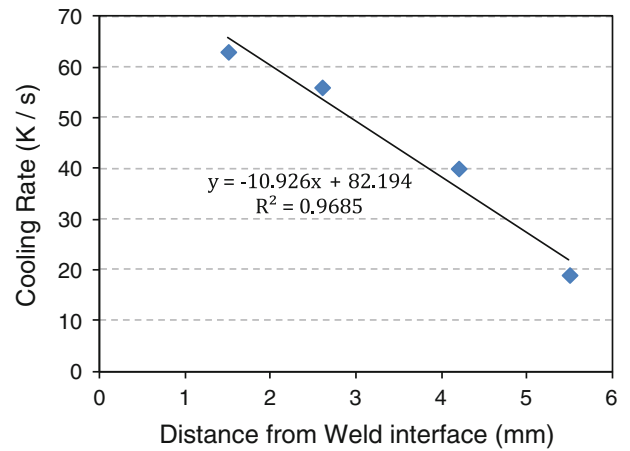
water tank. The minimum time required for quenching of the sample was measured to be about 4 seconds. Similarly, the very short quenching time of hot compressed samples do not allow for noticeable changes in the grain size. Therefore, constitutive equations developed by hot compression can be used reliably for LFW.

In order to estimate the strain rate during LFW of sample A, the measured grain size at the weld interface (13.1 μm) and estimated temperature, 1491 K (1218 °C), were implemented into Eq. [5b]. The calculation indicated that the strain rate is about 1520 s^{-1} in the weld area of weldment A. This value is relatively close to the one predicted by Turner *et al.*,[7] *i.e.*, 1325 s^{-1}, and much higher than the 18.5 s^{-1} calculated from Vairis and Frost equation (Eq. [6]).

For weldment B, the predicted grain size (21.6 μm) based on Eq. [5b] was significantly larger than the measured one (4.0 μm). This behavior can be understood in terms of the imposed deformation during each stage of LFW process. In sample B, in contrast to sample A, at the end of the oscillation phase, the forged pressure was increased from 1.3P to 4P (Table I). Under these conditions, as shown in Figure 9(b), significant amounts of deformation occurred during the forge phase. Thus, the temperature calculations and strain rate estimation from the Turner *et al.* study, which are exclusively for the estimation of temperature and strain rate at the end of the oscillation phase, cannot be used for the forge phase. In other words, the temperature and strain rate of the forge phase should *also* be estimated and implemented into the constitutive equation for a reliable prediction. The mathematical equations or FEM results for estimation of the temperature and strain rate in the forge phase of LFW are not available in the open literature and hence no comparison can be made at this stage.

E. *Reliability of the Predictions*

In order to evaluate the repeatability of the proposed approach, the measured grain size at the weld interface

of another weldment (C) with an axial shortening of 1.75 mm was compared with the predicted value. For this sample, the interface temperature was calculated to be 1523 K (1250 °C), and the strain rate was estimated to be 1325 s^{-1}. The predicted grain size (15.6 μm) was very close (4.6 pct difference) to the measured one (14.9 μm) using Eq. [5b]. In this sample, almost the entire deformation was applied in the oscillation phase, and no increase in the forge pressure was made after the oscillation phase (similar to sample A). The above analysis clearly validates the reliability of the approach used in the current study for predicting the grain size evolution in the weld area of the LFWed Waspaloy when the forged pressure is not changed.

IV. CONCLUSIONS

In the current study the evolution of the grain size and strain rate in the weld area of LFWed Waspaloy was successfully modeled using hot compression testing carried out in the 1333 K to 1413 K (1060 °C to 1140 °C) temperature range, 0.001 to 1 s^{-1} strain rate range, and up to a strain of 0.83. Since γ' is the main phase for grain size control during processing, complete dissolution of these particles before starting the deformation resulted in grain growth from 10 to 211 μm. DRX occurred during hot deformation and resulted in flow softening. The activation energy for hot deformation of Waspaloy in the supersolvus temperature range was estimated to be 462 kJ/mol. The constitutive equations developed from hot compression experiments were used to predict the grain size and strain rate in LFWed Waspaloy. The grain size of the LFWed Waspaloy can be reliably determined using the constitutive equations with determination errors of less than 5 pct for the experimental conditions studied in the current study. It was predicted that strain rate in the weld area of LFWed Waspaloy was in the range of 1520 s^{-1}.

REFERENCES

1. R.E. Bailey: *2nd Int. Conf. on Superalloys-Processing*, Seven Springs, PA, Battelle Columbus Labs., Columbus, OH, 1972, pp. J1–J21.
2. A. Chamanfar, M. Jahazi, J. Gholipour, P. Wanjara, and S. Yue: *Metall. Mater. Trans. A*, 2011, vol. 42A, pp. 729–44.
3. A.K. Abdul Jawwad, M. Strangwood, and C.L. Davis: *Metall. Mater. Trans. A*, 2003, vol. 34A, pp. 1637–45.
4. V. Siva Kumar, G. Kelekanjeri, and R.A. Gerhardt: *Electrochim. Acta*, 2006, vol. 51, pp. 1873–80.
5. Technical Data Sheet, Allegheny Technologies Incorporated (ATI), Pittsburgh, PA, 2009.
6. I. Bhamji, M. Preuss, P.L. Threadgill, and A.C. Addison: *Mater. Sci. Technol.*, 2011, vol. 27, pp. 2–12.
7. R. Turner, J.-C. Gebelin, R.M. Ward, and R.C. Reed: *Acta Mater.*, 2011, vol. 59, pp. 3792–3803.
8. A. Vairis and M. Frost: *Wear*, 1998, vol. 217, pp. 117–31.
9. A.A. Guimaraes and J.J. Jonas: *Metall. Trans. A*, 1981, vol. 12A, pp. 1655–66.
10. H.J. McQueen, G. Gurewitz, and S. Fulop: *High Temp. Technol.*, 1983, vol. 1, pp. 131–38.
11. S.L. Semiatin, D.S. Weaver, P.N. Fagin, M.G. Glavicic, R.L. Goetz, N.D. Frey, R.C. Kramb, and M.M. Antony: *Metall. Mater. Trans. A*, 2004, vol. 35A, pp. 679–93.
12. G. Shen, S.L. Semiatin, and R. Shivpuri: *Metall. Mater. Trans. A*, 1995, vol. 26A, pp. 1795–1803.
13. A. Chamanfar, M. Jahazi, J. Gholipour, P. Wanjara, and S. Yue: *Mater. Sci. Eng. A*, 2012, vol. 555, pp. 117–30.
14. S. Xu, J.I. Dickson, and A.K. Koul: *Metall. Mater. Trans. A*, 1998, vol. 29A, pp. 2687–95.
15. S. Olovsjö, A. Wretland, and G. Sjöberg: *Int. J. Adv. Manuf. Technol.*, 2010, vol. 50, pp. 907–15.
16. B. Lindsley and X. Pierron: in *Superalloys 2000*, T.M. Pollock, R.D. Kissinger, R.R. Bowman, K.A. Green, M. McLean, S. Olson, and J.J. Schirra, eds., TMS, Warrendale, PA, 2000, pp. 59–68.
17. ASTM Standard E 562-02, *Annual Book of ASTM Standards*, ASTM, Philadelphia, PA, 2002, vol. 3 (1), pp. 1–7.
18. H. Monajati, M. Jahazi, S. Yue, and A.K. Taheri: *Metall. Mater. Trans. A*, 2005, vol. 36A, pp. 895–905.
19. A.R. Mashreghi, H. Monajatizadeh, M. Jahazi, and S. Yue: *Mater. Sci. Technol.*, 2004, vol. 20, pp. 161–66.
20. S.C. Medeiros, Y.V.R.K. Prasad, W.G. Frazier, and R. Srinivasan: *Mater. Sci. Eng. A*, 2000, vol. 293, pp. 198–207.
21. Y.-S. Na, S.-J. Choe, and N.-K. Park: *The International Symposium on Hot Workability of Steels and Light Alloys-Composites*, Montreal, Canada, 1996, pp. 227–36.
22. J.P. Hu, J.Y. Zhuang, J.H. Du, Q. Deng, D. Feng, Z.Y. Zhong, P. Janschek, and J. Kramer: *Acta Metall. Sin.*, 2001, vol. 14, pp. 205–211.